IOP Conf. Series: Materials Science and Engineering **181** (2017) 012043 doi:10.1088/1757-899X/181/1/012043

Influence of the heat treatment condition of alloy AlCu4Mg1 on the microstructure and properties of anodic oxide layers

R Morgenstern, D Dietrich, M Sieber and T Lampke

Institute of Materials Science and Engineering, Chemnitz University of Technology, 09125 Chemnitz, Germany

Abstract. Due to their outstanding specific mechanical properties, high-strength, age-hardenable aluminum alloys offer a high potential for lightweight security-related applications. However, the use of copper-alloyed aluminum is limited because of their susceptibility to selective corrosion and their low wear resistance. These restrictions can be overcome and new applications can be opened up by the generation of protective anodic aluminum oxide layers. In contrast to the anodic oxidation of unalloyed aluminum, oxide layers produced on copper-rich alloys exhibit a significantly more complex pore structure. It is the aim of the investigation to identify the influence of microstructural parameters such as size and distribution of the strengthening precipitations on the coating microstructure. The aluminum alloy EN AW-2024 (AlCu4Mg1) in different heat treatment conditions serves as substrate material. The influence of the strengthening precipitations' size and distribution on the development of the pore structure is investigated by the use of high-resolution scanning electron microscopy. Integral coating properties are characterized by non-destructive and light-microscopic thickness measurements and instrumented indentation tests.

1. Introduction

Due to their high specific strength, aluminum alloys are widely used as lightweight construction materials. The outstanding mechanical properties of the age-hardenable aerospace alloy EN AW-2024 (AlCu4Mg1) are related to the precipitation of microstructural heterogeneities. According to Sha et al. [1], copper- and magnesium-rich atomic clusters and Guinier-Preston-Bagaryatsky zones (GPB zones) crucially influence the mechanical strength. Furthermore, rod-shaped Al_2CuMg precipitates (S-phase), Al_2Cu precipitates with different degree of coherence and lattice structures as well as different nanoscale iron-, silicon- and manganese-containing precipitates develop during artificial aging at higher temperatures [2]. In general, the open circuit potential (OCP) of intermetallic phases (IMPs) and the surrounding aluminum solid solution (Alss) are different. In the presence of an electrolyte, the potential difference leads to the selective electrochemical corrosion of the less noble phases.

Aluminum alloys can be efficiently protected from corrosion by the electrochemical conversion of the aluminum substrate surface into an anodic aluminum oxide (AAO) layer. The development of an ordered hexagonal pore-structure during the anodic oxidation process has already been described by Keller et al. [3] in 1953. Recent studies describe the effect of alloying elements and impurities on the anodic oxidation of high-strength aluminum alloys. For copper-containing alloys, the influences of highly-dispersed copper atoms and copper-rich intermetallic phases can be differentiated. Copper atoms in solid solution accumulate to copper-rich particles at the substrate-oxide interface due to the preferential oxidation of aluminum atoms. The anodic overpotential at the interface increases with the depletion of aluminum atoms enabling the oxidation of copper-rich particles. In contrast to aluminum

oxide, copper oxide is an electronic conductor which allows for the evolution of oxygen gas bubbles at the anode. As copper enrichment and oxidation repeat periodically, the ordered pore-structure is superimposed by repetitive gas-voids [4]. According to Ma et al. [5], microscale copper-rich IMPs such as Al_2CuMg are rapidly anodically dissolved as soon as they get in contact with the electrolyte, because the copper-rich oxide formed at the IMP's surface is not electrochemically stable in the electrolyte. After rapid dissolution of the IMPs, microscale cavities remain within the AAO layer.

In naturally and artificially aged conditions, which are of high technical importance, the degree of copper segregations lies in between the highly dispersed state (copper in solid solution) and the thermodynamic equilibrium state (microscale S-phase precipitates). It is the aim of this work to clarify, at which point of copper segregation a different microstructure of AAO layers is observed and to what extent the macroscopic coating properties are influenced.

2. Material and methods

Sheets of the aluminum alloy EN AW-2024 (chemical composition in wt%: 3.8–4.9 Cu, 1.2–1.8 Mg, 0.3–0.9 Mn, ≤0.5 Si, ≤0.5 Fe, ≤0.1 Cr, ≤0.25 Zn, ≤0.15 Ti) with dimensions of 50x25x1,5 mm³ were used as substrate material. All sheets were solution annealed (505 °C, 1 h) and quenched in water, immediately followed by pretreatment and anodization (condition W), natural aging (room temperature, > 14 days, condition T4), peak aging (180 °C, 16 h, condition T6), overaging (220 °C, 20 h, condition T7).

Sample pretreatment included etching in 3 wt% sodium hydroxide at 50 °C for 5 min and pickling in 1:1 nitric acid at room temperature for 30 s. Each step was followed by rinsing under deionised water. The anodic oxidation was conducted at 22 °C (room temperature) and 5 °C in 20 vol% sulphuric acid (Merck, Germany) at a constant current density of 2 A/dm² for a duration of 1 hour. The coating thickness was measured by non-destructive eddy-current testing (Fischerscope MMS) as well as by optical microscopy on cross-sections.

Metallographic cross-sections were prepared by diamond grinding accomplished by a finish using a silica oxide polishing suspension. The microstructure was investigated by scanning electron microscopy (SEM, Zeiss, LEO 1455VP) and field emission scanning electron microscopy (FE-SEM, Zeiss, NEON40EsB). Both secondary electron (SE, topography contrast) and backscattered electron (BSD, element contrast) detectors were applied. Hardness profiles of the AAO cross-sections were measured by nanoindentation (UNAT) using a Berkovich indenter and a normal load of 5 mN.

3. Results and discussion

3.1 Substrate and coating microstructure

During solidification of EN AW-2024 alloy, iron and silicon rich intermetallic phases precipitate from the liquid phase. Because of the low solubility of iron and silicon in the Alss even at high temperatures, these primary phases remain largely unchanged after solution annealing and quenching. Also, microscale Al_2CuMg precipitates, which formed due to slow cooling, are not completely solved during one hour of solution annealing. The complete dissolution of this phase would require a significantly longer annealing time, which leads to undesirable grain coarsening. However, this phase is partly dissolved and formed to a spherical or ellipsoidal shape.

As shown in figure 1, the iron- and silicon-rich primary precipitates mostly exhibit an irregular elongated shape due to previous sheet processing. After anodizing, these precipitates leave highly porous areas within the AAO layer. As described above, the spherical Al_2CuMg precipitates are rapidly dissolved as soon as they get in contact with the electrolyte. Thus, they leave microscale spherical cavities within the conversion layer. The different coating properties described below are not caused by these microscale defects as they can be observed in the AAO layers of all heat treatment conditions.

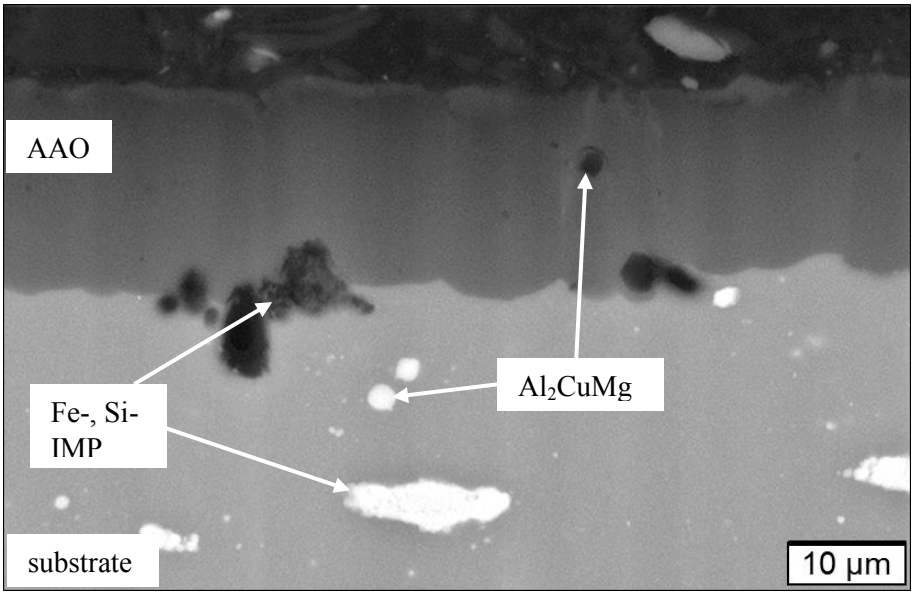

Figure 1. Microscale precipitations in the substrate leading to microscale defects within the AAO layer (SEM, BSD picture).

Clusters of copper and magnesium atoms already precipitate some hours after solution annealing and water quenching from the supersaturated Alss [1]. The microstructures of the heat treatment conditions W and T4 differ in respect of the size and number of clusters as well as of the amount of copper and magnesium remaining in solid solution. However, as atomic clusters cannot be recognized at FE-SEM pictures because of their small size, the substrate microstructure of the condition T4 is also representative for the condition W. As shown in the BSD picture figure 2a, the condition T4 exhibits bright spheroidal precipitates, which contain heavier elements than aluminum, e.g. iron, silicon or manganese. After the anodic oxidation, these precipitates leave spheroidal pores or highly porous areas within the AAO layer. However, the microstructure of the AAO layer is determined by cyclic enrichment of highly dispersed copper at the substrate-coating interface and the oxidation of copper rich particles being accompanied by oxygen evolution. As described above, this leads to the formation of fine gas voids along the ordered pore channels (figure 3a).

Artificial aging at 180 °C (peak-aged condition T6) leads to the development of a network of bundled GPB zones in the substrate alloy (figure 2b). Due to the higher copper content of these zones, a more porous and less stable oxide is formed leading to a stronger dissolution. At the SE image of the AAO cross-section (figure 3b), these porous areas appear as wells. Between the wells, a porous microstructure similar to the conditions T4 and W can be observed. Consequently, a sufficient amount of highly dispersed copper atoms or clusters exists between the GPB zones leading to copper enrichment at the substrate-coating interface and the cyclic generation of gas voids.

During artificial aging at 220 °C (overaged condition T7), the precipitation of the S-phase at grain boundaries is more pronounced. Some grain boundaries as well as two triple junctions appear as bright "dotted" lines in figure 2c (element contrast) due to the copper rich precipitates. Within close proximity of the S-phase, e.g. around grain boundaries, areas with a dark appearance indicate a local copper depletion. This observation is confirmed by the findings of Sha et al. [1]. In contrast to the GPB zones in condition T6, the rod-like S-phase precipitates in the grain interior exhibit a higher material contrast and a stricter orientation to one another. Some of the numerous bright spheroidal phases in figure 2c might be assignable to the Ω-phase being another modification of Al_2CuMg, which typically forms at temperatures above 200 °C [2].

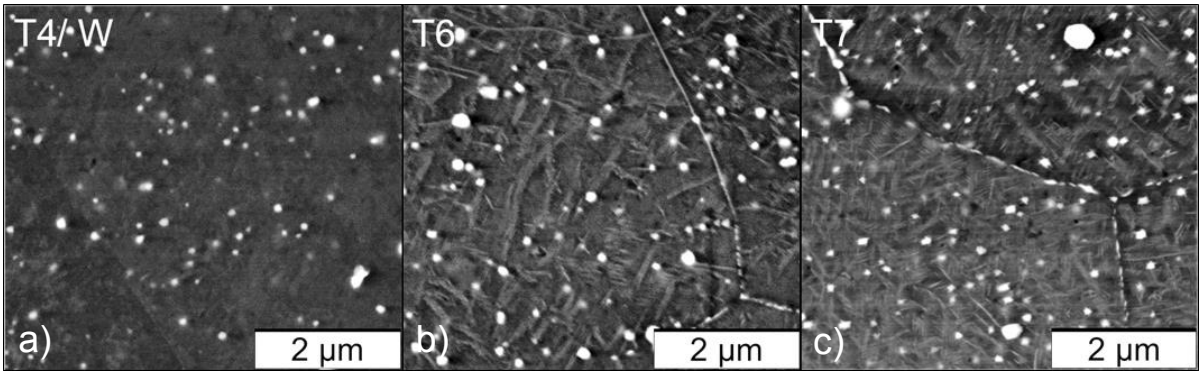

Figure 2. Microstructure of alloy EN AW-2024 in heat treatment conditions T4/W (a), T6 (b) and T7 (c) (FE-SEM, BSD).

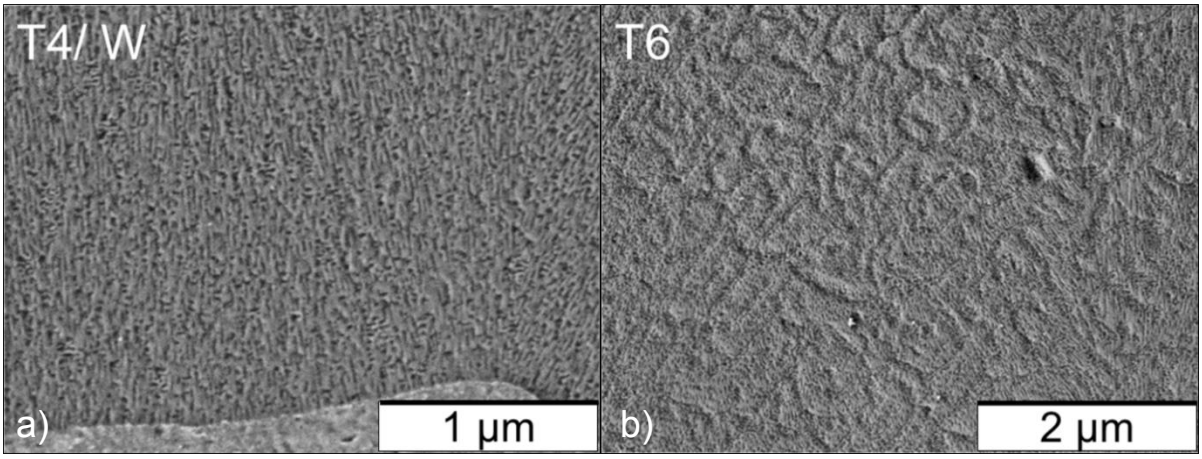

Figure 3. Microstructures of AAO coatings on alloy EN AW-2024 in heat treatment conditions T4/W (a), T6 (b) after anodizing at 22 °C (FE-SEM, SE).

Similar to microscale S-phase precipitates, the fine S-phase rods in the overaged condition leave cavities in the AAO layer after room temperature anodizing due to their rapid dissolution in the electrolyte. In the coating cross section (figure 4a), these cavities appear as elongated wells within the former grain interior and along the former grain boundaries. Areas of the AAO in close vicinity of the elongated wells appear to be less porous in comparison with the AAO microstructure of the conditions W and T4. The formation of additional gas voids along the ordered pore channels cannot be observed there. This finding correlates with the copper depletion in the surrounding of S-phase precipitates. During anodic oxidation of these depleted areas, no significant copper enrichment takes place at the substrate-coating interface and no significant oxygen evolution takes place at the alumina barrier layer. Again, some ellipsoid pores are visible within the coating. They might be attributable to the dissolution of the Ω-phase.

Similar to room temperature anodizing, hard anodizing of the conditions T4 and W at 5 °C is also characterized by the cyclic copper enrichment and oxidation at the substrate-coating interface leading to the cyclic formation of small gas voids. However, the influence of the heat treatment condition on the coating microstructure is less pronounced. As shown in figure 4b, elongated areas containing fine gas voids can be observed next to more compact areas with an ordered pore structure. In contrast to room temperature anodizing of condition T7 (figure 4a), the porous areas exhibit less topography contrast.

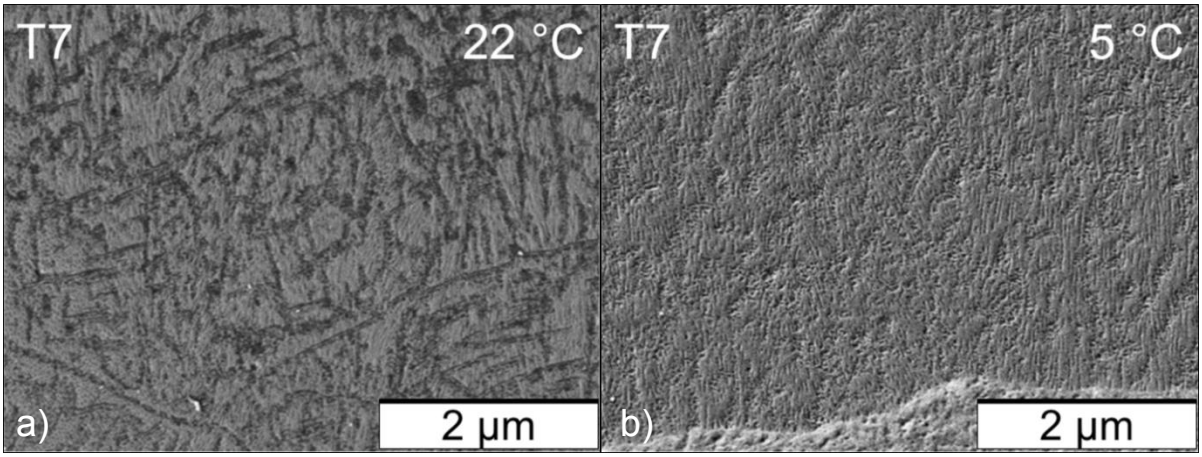

Figure 4. Microstructures of AAO coatings on alloy EN AW-2024 T7 after anodizing at 22 °C (a) and at 5 °C (b) (FE-SEM, SE).

3.2 Coating properties

It can be seen from figure 5a that for room temperature anodizing the coating thickness strongly depends on the heat treatment condition. Although an identical charge quantity of 2 Ah/dm² (and also approx. the same potential of about 13 V) was applied to all samples, conditions W and T4 exhibit the lowest coating thicknesses of about 18 to 19 µm. This might be due to the oxygen evolution, which occurs at the substrate-coating interface as a result of the cyclic enrichment and oxidation of copper. As electrical charge is consumed by this side-reaction, the current efficiency of the oxide formation and thus the coating thickness decrease. With increasing segregation of the alloying elements (clusters → GPB zones → S-phase) the thickness of the AAO layer increases. Possibly, chemical dissolution takes part during the rapid dissolution of the S-phase to a greater extent as the copper-rich oxide is not stable in the sulfuric acid electrolyte. Consequently, oxygen evolution is reduced due to the smaller amount of electrochemical dissolution. As no significant oxygen evolution takes place during the oxidation of copper-depleted regions, the highest current efficiency and coating thickness can be observed for condition T7. The anodizing behavior of condition T6 can be seen as an intermediate between T4 and T7, therefore it is consistent that the coating thickness also lies in between.

In general, higher coating thicknesses are achieved at 5 °C as the chemical dissolution of the AAO is smaller. However, the chemical dissolution of copper-rich regions such as the S-phase also decreases significantly. Consequently, electrochemical processes dominate the dissolution of the S-phase and the oxygen evolution is more pronounced. In contrast, less oxygen evolution takes place during the oxidation of copper-depleted areas. In total, the different extents of oxygen evolution seem to compensate one another. Consequently, the anodization of heat treatment conditions with both high copper segregation and high copper dispersion take place with a similar current efficiency. For all heat treatment conditions the coating thickness amounts to about 40 µm.

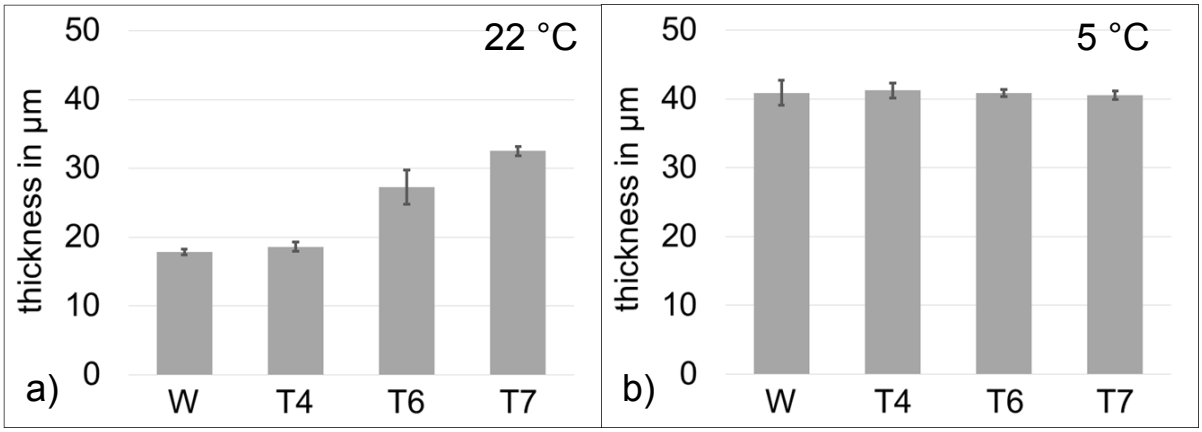

Figure 5. Coating thicknesses after anodizing of different heat treatment conditions at a) 22 °C, b) 5 °C.

The measured hardness values include the hardness of compact AAO and pores and therefore correlate with the average coating porosity of the examined volume. As the pore channel diameter enlarges with increasing exposition time in the electrolyte due to chemical dissolution, the hardness generally decreases with increasing distance from the substrate. This especially applies to room temperature anodizing because of the increasing reactivity of the sulphuric acid electrolyte at higher temperatures. In order to illustrate the typical deviation of hardness values for room temperature anodization, figure 6a shows all measuring points for the condition T7. It can be seen that the trendlines for conditions W and T4 are in the same range correlating with the similar coating microstructure. Compared with this, the trendline for condition T7 lies at a higher level which implies that the heterogeneous microstructure consisting of compact areas and elongated cavities (see figure 4a) exhibits a lower global porosity and thus a higher global hardness than the homogeneous coating microstructure of the conditions W and T4 being characterized by numerous small gas voids (see figure 3a). The hardness profile of AAO coatings on condition T6 lies in between those of conditions W/ T4 and T7, which corresponds with the intermediate heterogeneity of the coating microstructure. For hard anodizing, only a slight influence of the heat treatment condition on the AAO hardness can be observed. As can be seen from figure 6b, the single hardness points for conditions W and T7 partly overlap one another and the trendlines are close together. This again corresponds with the minor microstructural differences between AAO coatings on the conditions W/ T4 and T7 after hard anodizing.

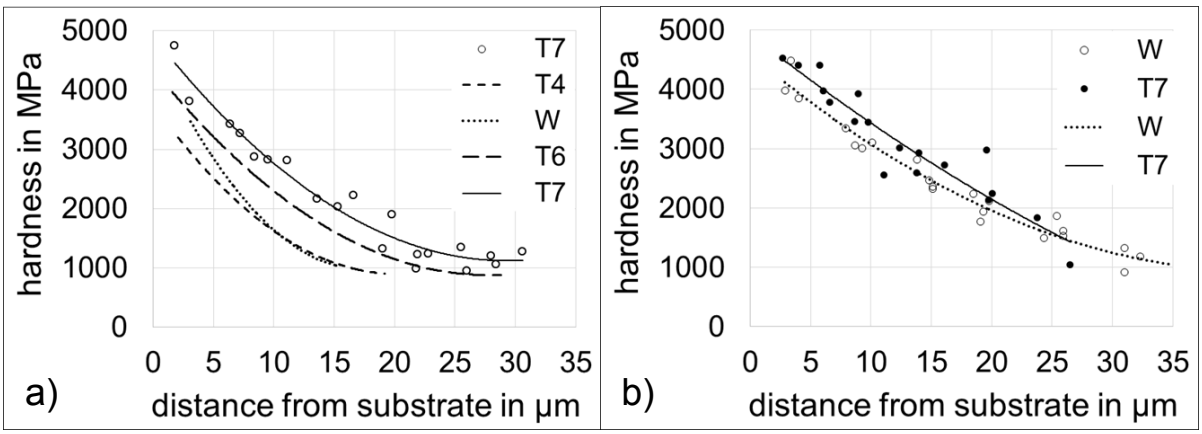

Figure 6. Hardness profiles of AAO coatings on different heat treatment conditions after anodizing at a) 22 °C and b) 5 °C.

4. Conclusions

It was shown that for room temperature anodizing the microstructure and the macroscopic properties of AAO coatings significantly depend on the heat treatment condition of the substrate alloy AlCu4Mg1. In case that alloying elements are highly dispersed within the substrate (e.g. in Alss or atomic clusters), oxygen evolution takes place at the substrate-coating interface due to the cyclic enrichment and oxidation of copper. This leads to the formation of fine gas voids along the ordered pore channels as well as to the reduction of the current efficiency of oxide formation and thus to a reduction of the coating thickness. After artificial aging, the segregation of copper increases and copper-depleted regions develop next to copper-rich precipitates such as the S-phase. As no significant copper enrichment takes place during the anodization of copper depleted regions, no significant oxygen evolution and void formation occurs. The S-phase rapidly dissolves during anodizing due to electrochemical dissolution and the chemical attack of the electrolyte leaving elongated cavities in the AAO layer. Therefore, less oxygen evolution occurs during room temperature anodization of the condition T7 resulting in higher current efficiency and coating thickness. The heterogeneous AAO microstructure consisting of compact regions and elongated cavities exhibits a higher hardness than the homogeneous AAO microstructures of conditions W and T4.

Basically, the same mechanisms of AAO formation apply to room temperature and hard anodizing at 5 °C for the conditions W and T4. However regarding the condition T7, the chemical dissolution of copper-rich regions such as the S-phase is less emphasized as the reactivity of the electrolyte decreases with lower temperature. As a result, the oxygen evolution is not reduced significantly and the current efficiencies for the anodization of different heat treatment conditions are similar. Consequently, coating properties like thickness and hardness are not significantly influenced by the heat treatment condition for hard anodizing.

It can be concluded from these results that for industrial room temperature anodizing of alloy AlCu4Mg1, process conditions have to be adjusted for different heat treatment conditions in order to fulfill coating specifications economically, e.g. a specific coating thickness can be achieved in a shorter process time on condition T7 compared with condition T4. Regarding hard anodizing, different heat treatment conditions might be anodized within the same process with the objective of optimizing the throughput as thickness and hardness of AAO coatings do not vary significantly.

Acknowledgement

The authors gratefully acknowledge funding by the German Research Foundation (Deutsche Forschungsgemeinschaft, DFG) within the framework of the Collaborative Research Centre 692 (SFB HALS 692, subproject B2). The technical assistance of J. Xu, D. Spieler, K. Muhr and C. Gläser is also gratefully acknowledged.

References

[1] Sha G, Marceau R K W, Gao X, Muddle B C and Ringer S P 2011 *Acta Mater.* **59** 1659
[2] Zhang F, Levine L E, Allen A J, Campbell C E, Creuziger A A, Kazantseva and Ilavsky J 2016 *Acta Mater.* **111** 385
[3] Keller F, Hunter M S and Robinson D L 1953 *J. Electrochem. Soc.* **100** 411
[4] Curioni M, Roeth F, Garcia-Vergara S J, Hashimoto T, Skeldon P, Thompson G E and Ferguson J 2010 *Surf. Interface Anal.* **42** 234
[5] Ma Y, Zhou X, Thompson G E, Curioni M, Zhong X, Koroleva E, Skeldon P, Thomson P and Fowles M 2011 *Corros. Sci.* **53** 4141